Arch. Metall. Mater. **66** (2021), 4, 1033-1036

DOI: 10.24425/amm.2021.136420

CHEOL-WOO KIM[1], HYO-SANG YOO[1], JAE-YEOL JEON[1],
KYUN-TAEK CHO[1], SE-WEON CHOI[1*]

STUDY ON IMPROVEMENT OF SURFACE PROPERTIES OF LOW CARBON STEEL USING LASER CLADDING

Laser cladding is a method that can be applied to repair the crack and break on the mold and die surfaces, as well as generate new attributes on the surface to improve toughness, hardness, and corrosion resistance. It is used to extend the life of the mold. It also has the advantages of superior bonding strength and precision coating on a local area compared with the conventional thermal spraying technology. In this study, we investigated the effect of cladding on low carbon alloy steel using 18%Cr-2.5%Ni-Fe powder (Rockit404), which showed high hardness on the die surface. The process conditions were performed in an argon atmosphere using a diode laser source specialized for 900-1070 nm, and the output conditions were 5, 6, and 10 kW, respectively. After the cladding was completed, the surface coating layer's shape, the hardness according to the cross-section's thickness, and the microstructure were analyzed.

Keywords: Laser cladding, Vickers hardness, Microstructure, Surface treatment

1. Introduction

TP23P40 is the low carbon steel with a slight modification of the chemical elements of AISI P20 and ASTM A681 P20. It is a commonly used die material for plastic injection molding applications because of its excellent mirror polishing, wear resistance, and corrosion resistance.

The main causes of damage or breakdown of this material under actual service conditions are wear, erosion, and thermo-mechanical fatigue, which may require immediate repair or replacement of the entire part [1-4]. The laser cladding method has recently been applied to repair damaged parts or surfaces to accurately improve these disadvantages. Precise repair of damaged areas or surfaces is much more cost-effective than a full replacement. Laser cladding can be applied to a remanufacturing process, especially for repairing cracks in the mold and dies surface [5-7]. It increases the mold's life by creating new properties on the substrate surface to improve toughness and hardness. This study investigates the effect of laser parameter on 18%Cr-2.5%Ni-Fe powder (Rockit404) cladding onto plastic die steel to exhibit high surface hardness properties. Chemical composition, metallurgical bonding between the clad layer and substrate, and the clad layer's hardness are presented.

2. Experimental

The Rockit401(18%Cr-2.5%Ni-Fe powder) cladding samples were fabricated on low carbon steels TP23P40 with 200×100×10 mm dimensions. Substrates were ground with a scouring wheel and degreased with acetone before the cladding process to improve the surface's laser absorptivity. Typical chemical composition of Rockit401 (Fe-0.5wt.%C-18wt.%Cr-0.5wt.%Mo-2.5wt.%Ni) and TP23P40 (Fe-0.42wt.%C-1.0wt.%Mn-0.3wt.%Si-1.0wt.%Cr-0.23wt.%Mo) steel are presented in Table 1. The alloy powder used in laser cladding was Rockit401 powder with spherical morphology having an average particle size of 135 μm. Fig. 1 shows the morphology and size distribution of the powder used in the present study.

TABLE 1

Details of the experimental settings

Laser Power P(KW)	Cladding Speed V(m·min^{-1})	Heat Input Q(KJ/min)	Overlap Ratio for Multiple Beads (%)
5	0.42	12	63.9
6	0.42	14	63.9
10	0.42	24	63.9

[1] SMART MOBILITY MATERIALS AND COMPONENTS R&D GROUP, KOREA INSTITUTE OF INDUSTRIAL TECHNOLOGY, 1110-9 ORYONG-DONG, BUK-GU, GWANGJU, REPUBLIC OF KOREA

* Corresponding author: choisw@kitech.re.kr

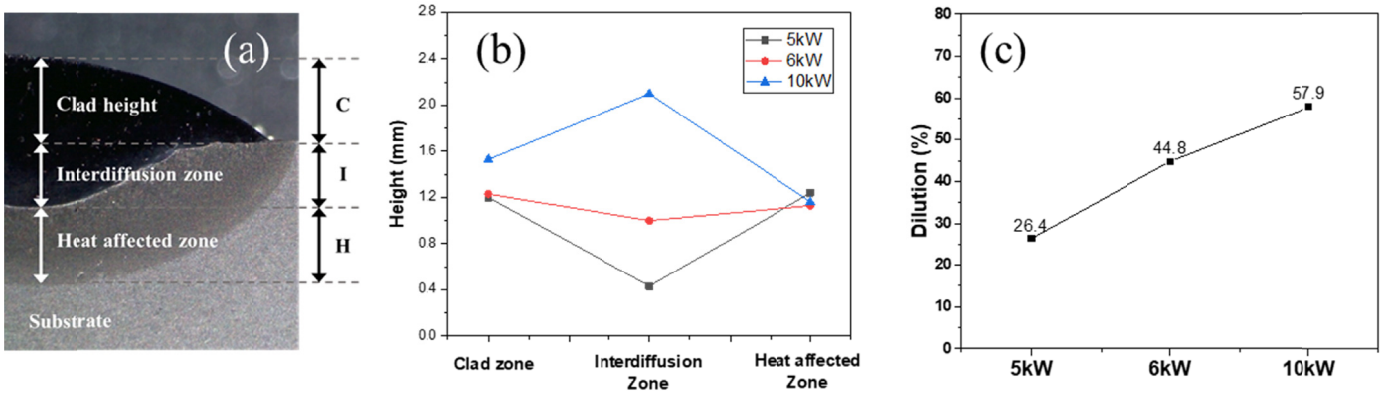

Fig. 1. The cross-sectional image of laser-cladded specimen (a) showing distinct three areas – (1) clad, (2) interdiffusion, and (3) heat affected zone – coating height (b) corresponding to distinct area (a), and dilution rate (c) with various laser powers, 5, 6, 10 kW

Laser cladding was carried out using a solid laser system (Laserline LDF10000-100). A 10 kW diode laser was coupled with fiber delivery, and the optical head system mounted on a 7-axis robot. The laser source was characterized by 900-1070 nm. The laser spot size was 8.3 mm with 1500 μm laser fiber core, 72 mm collimation lenses, and 400 mm focusing lenses. The experiment was performed in an argon (Ar) atmosphere. The distance between the coaxial powder feeding head and the surface of the substrate was 20 mm. The powder feeding gas (Ar) was 15 L/min, and all the powder feeding rate was 30.4 g/min. In order to exclude the facility variables, heat input value was chosen and calculated by using the cladding parameters. With the hatch spacing of 3 mm, overlap ratio at multiple beads was 63.9%. The laser cladding conditions and geometrical parameters of the resulting single beads are summarized in Table 1.

The heat inputs for each set of parameters were also compared according to the following equation.

$$Q = \frac{P(\mathrm{W})}{V(\mathrm{m/min})} \tag{1}$$

Where Q is the heat input; P is the laser power; V is the scanning speed.

All of the specimens were longitudinally cross-sectioned, ground by sandpaper, and polished with a diamond suspension of 3 μm and 1 μm. Silica suspension was used for fine polishing. Later, Rockit401 stainless steel was etched with aqua regia (nitric acid + hydrochloric acid) to observe the interdiffusion zone, and TP23P40 low carbon steel was etched with natal 5% solution (nitric acid + ethanol) to observe the heat-affected zone. The hardness test was carried out under the conditions of the Micro Vickers hardness tester Hv0.1, according to the thickness (0.1 mm intervals) of the cross-section.

The macromorphology, composition, and microstructure of each clad layer and bonding area were investigated using optical microscopy (OM), field emission scanning electron microscopy (FESEM), and electron probe micro analyzer (EPMA).

3. Results and discussion

3.1. Macroscopic morphology

The cross-sectional image of laser cladded specimen showing distinct three areas corresponding to distinct area is shown in Fig. 1. The coating schematic shown in Fig. 1(a) indicates all the measurements for analysis. The laser cladding shape is formed mainly by clad height, interdiffusion zone, and heat-affected zone. As shown in Fig. 1(b), there was no significant difference in the heat-affected zone's height according to the laser power. However, as the laser power increased to 5 kW, 6 kW, and 10 kW, the amount of melted powder increased, so the interdiffusion zone increased to 0.43, 1.00, and 2.10 mm, respectively. In general, as the laser power increases, the coating height, width, and melt depth increase almost linearly [8].

According to the following equation, the geometric definition of the dilution is shown in Fig. 3(d).

$$dilution(\%) = \frac{I}{C+I} \times 100 \tag{2}$$

Where I is interdiffusion zone height (mm); C is clad height (mm).

Dilution can be defined as the percentage of the surface layer's total volume contributed by its melting substrate. It is desirable to minimize the dilution rate with the substrate as much as possible in order not to degrade the characteristics of the abrasion and corrosion resistance on clad material [9-11]. Fig. 1(c) shows the dilution rate by laser power, and it can be seen that the dilution rate increases as the power increases.

3.2. Microscopic morphology

Fig. 2 shows the heat-affected zone and substrate's microstructure formed at the heat inputs of 5 kW, 6 kW, and 10 kW laser power. The heat-affected zones of the specimens with the heat inputs of 5 kW and 6 kW are composed of a mixture of upper bainite and lower bainite. The specimen with the heat input of 10 kW has a different structure divided into three areas. It is

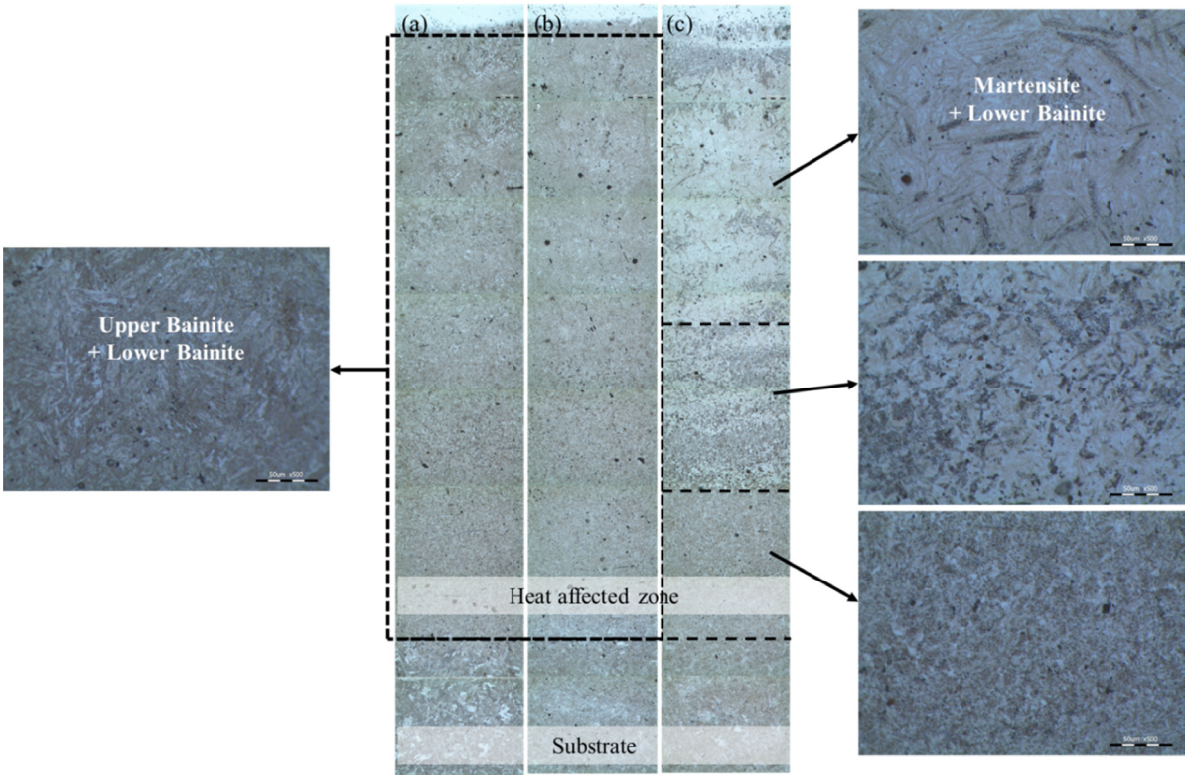

Fig. 2. OM images of Heat affected zone (HAZ) and Substrate material: (a) 5 kW, (b) 6 kW, and (c) 10 kW

composed of a mixture of martensite and lower bainite under the interdiffusion zone. Due to the high laser power, the melting temperature was very high, so that the austenite temperature was increased and then cooled, and martensite was present [12].

3.3. Micro-hardness distribution of the cladding layer

Fig. 3(a) shows the micro-hardness distributions along with the thickness in the cross-section of the cladding layers. It was measured at 0.1 mm intervals from the interdiffusion zone to the heat-affected zone. In the case of the interdiffusion zone, the micro-hardness increased with increasing at the laser power. It is considered to be due to the relatively high Mo content of 10 kW compared to 5 kW and 6 kW, as shown in the SEM/EDX results in Fig. 4.

In the heat-affected zone, the specimens with the heat inputs of 5 kW and 6 kW show no hardness changes according to cross-section depth and showed similar micro-hardness values to each other. On the other hand, the specimen with the heat input of 10 kW showed a high micro-hardness value at 0.4 mm distant from the interdiffusion zone. The hardness value of 10 kW decreased sharply as it closed to the substrate. The above results well corresponded to microstructure changes shown in Fig. 2. Fig. 3(b) shows the EPMA result of concentration distribution in the heat-affected zone. In the case of 5 kW, the concentration

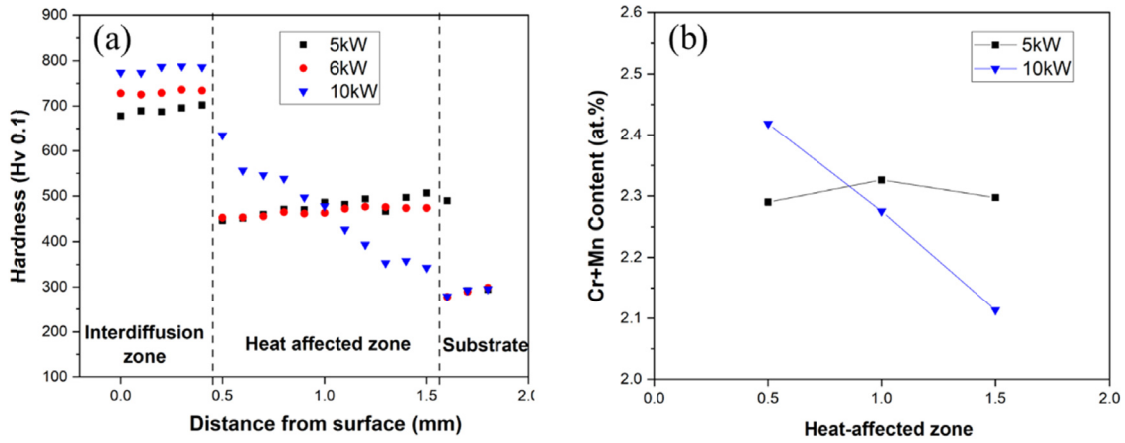

Fig. 3. Variations of micro-hardness with different laser powers and EPMA analysis of Heat affected zone (HAZ): (a) micro-hardness as a function of distance from top surface toward core matrix and (b) EPMA analysis results of HAZ on 5 kW and 10 kW

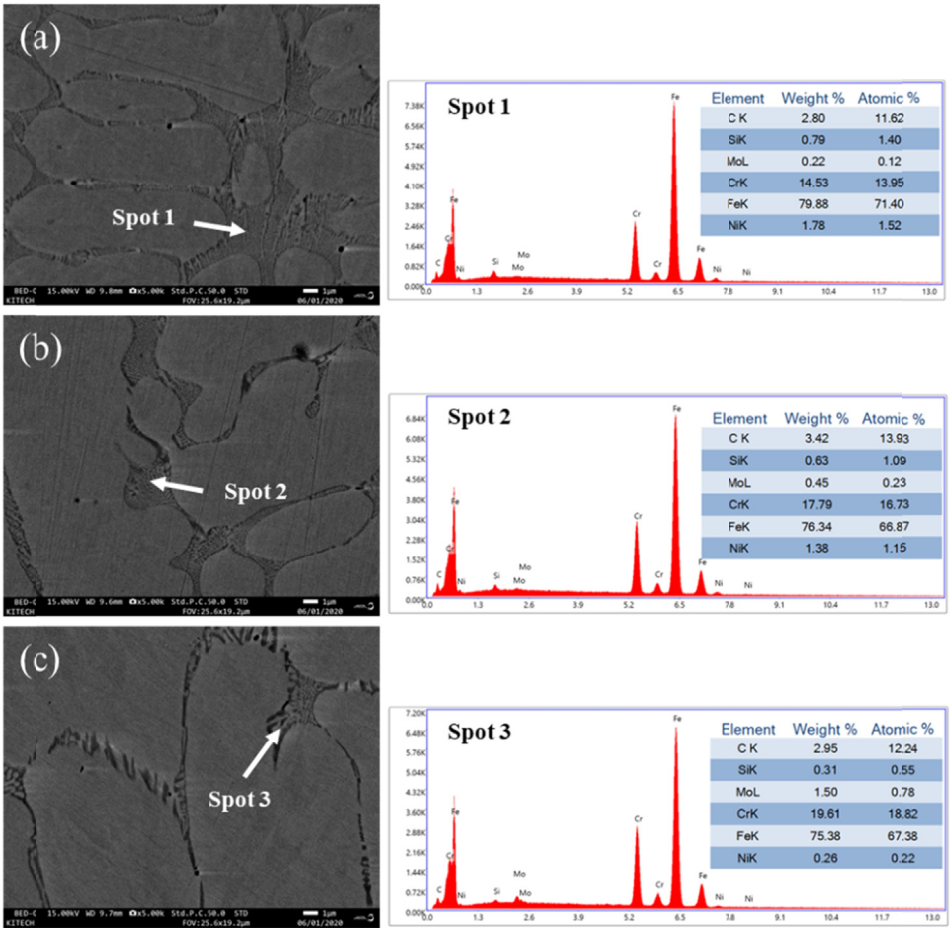

Fig. 4. SEM/EDX results of interdiffusion zone with different laser powers: (a) 5 kW, (b) 6 kW, (c) 10 kW

of Cr + Mn was constant regardless of the thickness of the heat-affected zone, while the concentration of 10 kW was higher than that of 5 kW. However, the closer to the substrate, the sharper the concentration of Cr + Mn decreased and was less than 5 kW in the 1.6 mm area. This result also explains the difference in hardness distribution according to laser power.

4. Conclusions

In this study, we investigated the effect of cladding on low carbon alloy steel using 18%Cr-2.5%Ni-Fe powder (Rockit404), which showed high hardness on the die surface. Obtained results are summarized as follows:

1. As a result of laser cladding with the heat inputs of 5 kW, 6 kW, and 10 kW, a sound clad layer was formed regardless of the laser power condition.
2. As the laser power increased from the heat input of 5 kW to 10 kW, the dilution rate of the cladding layer increased from 26.4 to 57.9%.
3. The microhardness distribution of the heat-affected zone of 0 ~ 0.5 mm in the depth direction just below the interdiffusion zone was higher in the case of 10 kW than that of 5 and 6 kW. This result was because of the higher the laser power, the higher the Cr + Mn concentration.

Acknowledgments

This research was a part of the project titled ‘The development of marine-waste disposal system optimized in an island-fishing village’, funded by the Ministry of Oceans and Fisheries of the Republic of Korea.

REFERENCES

[1] M. U. Saleem, Sustainability **10**, 1761 (2018).
[2] J. Tang, J. Egypro **5**, 708 (2011).
[3] N. Ali, J. Heliyon **6**, e05050 (2020).
[4] Y. Li, J. Jmrt **9**, 3856 (2020).
[5] P. Kattire, J. Jmapro. **20**, 492 (2015).
[6] Z. Zhang, J. Jallcom. **790**, 703 (2019).
[7] X. Xu, J. Jallcom. **715**, 362 (2017).
[8] G. Telasang, J. Surfcoat. **258**, 1108 (2014).
[9] J.H. Lee, J. KWJS **18**, 27 (2000).
[10] Z. Liu, J. Surfcoat. **384**, 125325 (2020).
[11] E.R. Mahmoud, J. Matpr. **39**, 1029 (2020).
[12] Y.T. Yoo, J. Korean Society **22**, 17 (2005).